IEEE Access
Multidisciplinary : Rapid Review : Open Access Journal

Received May 20, 2019, accepted June 25, 2019, date of publication June 28, 2019, date of current version July 16, 2019.

Digital Object Identifier 10.1109/ACCESS.2019.2925691

Novel Modulation Recognition for WFRFT-Based System Using 4th-Order Cumulants

YUAN LIANG[1], XIN XIANG[1], YE SUN[1], XINYU DA[2], CONG LI[1], AND LIYAN YIN[1]
[1]Aeronautics Engineering College, Air Force Engineering University, Xi'an 710051, China
[2]Information Engineering College, Yango University, Fuzhou 350000, China

Corresponding author: Yuan Liang (lycrazy0925@163.com)

This work was supported in part by the National Natural Science Foundation Program of China under Grant 61271250 and Grant 61571460, and in part by the National Postdoctoral Program for Innovative Talents under Grant 201700108.

ABSTRACT We present a novel modulation recognition for weighted-type fractional Fourier transform (WFRFT)-based systems using the fourth-order cumulants. First, the constellation characteristics of the basic digital modulations ASK, PSK, and QAM are analyzed, and the corresponding relationships between the neighboring constellation points' distance and the constellation size are deduced. Second, the closed-form expressions of the fourth-order cumulants (C_{42}) for the WFRFT-based systems with ASK, PSK, and QAM are derived. Finally, through the first- and second-order derivatives of the C_{42}, we prove that the optimal WFRFT order α_r can be obtained through the minimization of the C_{42}. The simulation results show that the novel recognition for the WFRFT-based system is feasible and can reach an accuracy of almost 90% when energy per bit-to-noise power spectrum density ratio (E_b/N_0) is greater than 6.

INDEX TERMS Weighted-type fractional Fourier transform (WFRFT), modulation recognition, order optimization using 4th-order cumulants.

I. INTRODUCTION

The Weighted-type Fractional Fourier Transform (WF-RFT) has become a promising communication technology since C.C. Shih firstly proposed it in 1995 [1]. The WFRFT-based system can be regarded as the convergence of Multi-Carrier (MC) and Single Carrier (SC) systems, and can be compatible with the current communication systems [2], [3], such as Single Carrier with Frequency Domain Equalization (SC-FDE), Orthogonal Frequency Division Multiplex(OFDM) and Long Term Evolution (LTE) [4]. The WFRFT-based system has the property to make the original signal bit energy distributed in frequency-time domain [2], and exhibits better performance on anti-interference [5]–[8] and anti-interception abilities [9]–[13] than other MC or SC systems. Since WFRFT-based system can be regarded as a novel hybrid carrier scheme that can converge the current SC and MC schemes [2], it's difficult to recognize the WFRFT signals by using the traditional recognition methods that apply to the SC and MC modulation recognitions. In addition, the modulation recognition is an important technology in the demodulation and further recovery of the received signal, especially when the communication systems are working in the non-cooperative way [14], [15]. However, there are few studies on the WFRFT modulation recognition. Thus, as for non-cooperative communication situations, finding an appropriate way to recognize WFRFT-based signals is a crucial issue that must be solved.

The modulation recognition methods can be classified into two categories: likelihood-based(LB) and feature-based(FB) methods [16]. By calculating the likelihood function of received signals for all modulation types, the LB algorithms can achieve accurate classification results, but also suffer from heavy computational cost [17]. The FB methods consist of two processes, namely, feature extraction and modulation classifier. And the classifier can identify different modulation types in accordance with the specific feature parameters extracted from the received signals [18]. As opposed to LB methods, the FB methods are computationally little, while may not be theoretically optimal [19]. Thus, more and more attention are paid to the FB methods. In the FB methods, kinds of features are extracted and have be validated effective on the modulation recognition, such as cyclic spectrum [20], cumulants [21], instantaneous features(amplitude, phase, and frequency) [22], and Gabor feature [23], etc. Among them, the signal statistics-based feature, especially the Higher

The associate editor coordinating the review of this manuscript and approving it for publication was Miaowen Wen.

Order Cumulants (HOC), owing to its inherent immunity to Gaussian noise [24], have gained many researcher's attention. And HOC has also been widely implemented in all kinds of communications, i.e. Multiple-Input and Multiple-Output (MIMO) [25], multi-path fading [26], Cognitive Radio(CR) [27], and satellite communications [28]. Thus, it's tempting to recognize the WFRFT-based signals based on HOC.

In [24], it has been proved that OFDM modulation does follow a Gaussian law and HOC of the OFDM modulated signals approach zero, which will not happen for SC modulated signals. The recognition methods based on HOC are often used to distinguish MC modulations from SC modulations. Considering that the WFRFT-based system can be adjusted flexibly between SC and MC systems when the WFRFT order α is set properly, we can't directly adopt the traditional modulation recognition methods based on HOC to recognize the WFRFT modulations. It has also been pointed out that there is a relationship between HOC and WFRFT order [29], whereas the quantitative relationship function hasn't been put forward. This paper mainly focuses on the quantitative relationship between HOC and WFRFT modulations, and detailed analyses are also carried out for different baseband modulations, such as ASK, PSK, and QAM.

This paper is organized as follows: In Section 2, the framework of WFRFT-based systems using 4th-order Cumulants is provided, and the related works about WFRFT are also put forward. In Section 3, the expressions of 4th-order Cumulants C_{42} with ASK, PSK, and QAM for WFRFT modulations are deduced. Through optimization theory, it has also been proved that the optimal WFRFT order α_r could be obtained through the minimization of C_{42}. In Section 4, numerical simulations are conducted to evaluate the performance of the proposed system. Conclusions and future works are drawn in the final section.

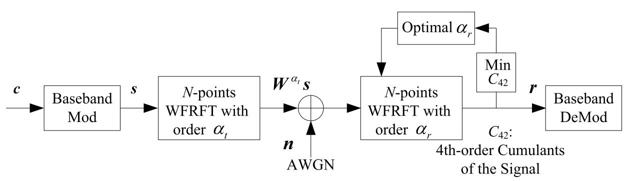

FIGURE 1. Framework of WFRFT-based systems using 4th-order cumulants.

II. FRAMEWORK OF WFRFT-BASED SYSTEMS

The basic framework of WFRFT-based systems is depicted in Fig. 1. After baseband modulation and α_t-th WFRFT, the original sequence $\boldsymbol{c} = [c_0, c_1, \cdots, c_{N-1}]^{\mathrm{T}}$ are transmitted in the Additive White Gaussian Noise(AWGN) channel. As for the receiving process, we calculate 4th-order Cumulants of the receiving signal and get the variable, C_{42}. By minimizing C_{42}, we can get the optimal α_r. Finally, we can recover the received signal through α_r-th WFRFT and baseband demodulation.

The classical 4-WFRFT of $\boldsymbol{X}_0$ can be described as [2]

$$\boldsymbol{W}^{\alpha}(\boldsymbol{X}_0) = \omega_0(\alpha)\boldsymbol{X}_0 + \omega_1(\alpha)\boldsymbol{X}_1 + \omega_2(\alpha)\boldsymbol{X}_2 + \omega_3(\alpha)\boldsymbol{X}_3, \quad (1)$$

where α is the WFRFT order, $\boldsymbol{X}_1, \boldsymbol{X}_2$ and $\boldsymbol{X}_3$ are the 1-3 times normalized Discrete Fourier Transform (DFT) of $\boldsymbol{X}_0$. And the expression of ω_l $(l = 0,\ 1,\ 2,\ 3)$ is given by [3]

$$\omega_l(\alpha) = \cos\left[\frac{(\alpha - l)}{4}\right]\cos\left[\frac{2(\alpha - l)}{4}\right]\exp\left[\frac{3(\alpha - l)j}{4}\right], \quad (2)$$

where j is the basic imaginary unit, and $j = \sqrt{-1}$.

Then in the form of matrix, the normalized WFRFT can be also expressed as

$$\boldsymbol{W}^{\alpha} = \omega_0(\alpha)\boldsymbol{F}^0 + \omega_1(\alpha)\boldsymbol{F}^1 + \omega_2(\alpha)\boldsymbol{F}^2 + \omega_3(\alpha)\boldsymbol{F}^3, \quad (3)$$

where $\boldsymbol{F}$ denotes the normalized DFT, the (m, n)-th element of which is given by

$$\boldsymbol{F}_{m,n} = \frac{1}{\sqrt{N}}\exp(-j2\pi mn/N),\ m, n = 0, 1, \cdots, N-1. \quad (4)$$

As shown in Fig. 1, we can write the received signal's expression as follows

$$r_k = \boldsymbol{W}_k^{\Delta\alpha}\boldsymbol{s} + \boldsymbol{W}_k^{\alpha_r}\boldsymbol{n},\ k = 0, 1, \ldots, N-1, \quad (5)$$

where, $\boldsymbol{s}$ is the baseband modulated sequence, $\boldsymbol{W}_k^{\Delta\alpha}$ is the k-th row of the normalized WFRFT matrix, and $\boldsymbol{n}$ is the AWGN vector($\boldsymbol{n} = [n_0, n_1, \cdots, n_{N-1}]^{\mathrm{T}}$). $\Delta\alpha$ denotes the WFRFT order offset, and $\Delta\alpha = \alpha_r + \alpha_t$. For the perfect receiving, $\Delta\alpha = 0$, that is, $\alpha_r = -\alpha_t$.

To describe the distribution properties of Gaussian distributed random variables n_k(the k-th element in $\boldsymbol{n}$), we use the short notation $n_k \sim N\left(\mu, \sigma^2\right)$, where μ and σ^2 are the expected value and the variance of n_k respectively. As the normalized WFRFT is a unitary linear transformation, $\boldsymbol{W}_k^{\alpha_r}\boldsymbol{n}$ has the same distribution properties with n_k, that is $\boldsymbol{W}_k^{\alpha_r}\boldsymbol{n} \sim N\left(\mu, \sigma^2\right)$ [30]. Then we can simplify the problem as the optimization program to minimize $\Delta\alpha$ in Eq.(5), which will be discussed in the next section.

III. THEORETICAL ANALYSES ON WFRFT-BASED SYSTEM

As for the digital communication system, ASK, PSK and QAM are the most commonly adopted. Related analyses on ASK, PSK, and QAM can provide a sound basis for other complex systems and communication situations. Then, our works mainly focus on the three modulations.

A. CONSTELLATION CHARACTERISTICS

In Fig.1, $\boldsymbol{c}$($\boldsymbol{c} = [c_0, c_1, \cdots, c_{N-1}]^{\mathrm{T}}$) are the original signal whose element $c_i, i = 0, 1, \cdots, N-1$ are generated from the integers between 0 and $M-1$. M is the modulation cardinality, i.e. the baseband constellation size. Usually, M should be an integer power of 2. For the three typical baseband modulations, ASK, PSK and QAM, the corresponding conversion

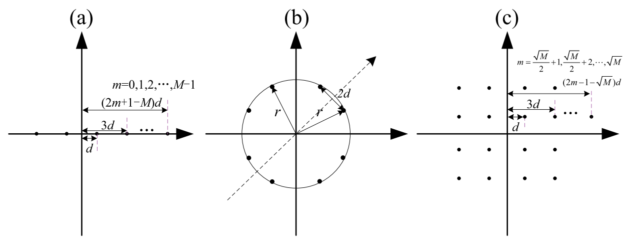

FIGURE 2. Diagram of the baseband modulation constellations: (a) ASK, (b) PSK, (c) QAM.

processes can be expressed by Eq.(6), (7) and (8) respectively. Then, as for the modulated signal $\boldsymbol{s}(\boldsymbol{s} = [s_0, s_1, \cdots, s_{N-1}]^{\mathrm{T}})$, according to the different baseband modulations, the element $s_i, i = 0, 1, \cdots, N-1$ can be generated based on Eq.(6),(7) and (8) respectively. When c_i is decided, there exists a unique s_i(equals to $\sqrt{S}x_i$,$\sqrt{S}y_i$ or$\sqrt{S}(p_i+jq_i)$) of the baseband modulation constellations in Fig.2. Fig. 2(a), (b) and (c) display the basic constellations of ASK, PSK, and QAM respectively. Let d be the basis distance unit. Then signals of these three baseband modulations can be expressed by [31]

$$\begin{aligned} X_{\mathrm{ASK}} &= \sqrt{S}x_i, x_i = (2m+1-M)d, \\ m &= 0, 1, \cdots, M-1, \qquad (6) \\ X_{\mathrm{PSK}} &= \sqrt{S}y_i, y_i = \exp\left(\frac{j2\pi(m-1)}{M}\right), \\ m &= 0, 1, \cdots, M-1, \qquad (7) \\ X_{\mathrm{QAM}} &= \sqrt{S}(p_i+jq_i), p_i, q_i = \pm(2m-1-\sqrt{M})d, \\ m &= \sqrt{M}/2+1, \sqrt{M}/2+2, \cdots, \sqrt{M}. \qquad (8) \end{aligned}$$

In Eq.(6), (7), and (8), S denotes the average power of the baseband signal, and M is the total number of the constellation points.

To make the average power of the signal equal to S, taking ASK for example, we can derive the basic distance unit, d_{ASK} for ASK

$$2 \cdot \left[1^2 + 3^2 + \cdots (M-1)^2\right] \cdot d_{\mathrm{ASK}}^2 \cdot S = M \cdot S. \qquad (9)$$

Then, according to the related sequence square summation formula, d_{ASK} is calculated by

$$d_{\mathrm{ASK}} = \sqrt{3/(M^2-1)}\,. \qquad (10)$$

Based on the same theory and methods, we can also derive the basic distance units for PSK and QAM [32]

$$\begin{aligned} d_{\mathrm{PSK}} &= \sin(\pi/M), \qquad (11) \\ d_{\mathrm{QAM}} &= \sqrt{3/\left[2(M-1)\right]}. \qquad (12) \end{aligned}$$

In Eq.(11), we assume $M \geq 4$ mainly because it is the same with 2ASK when $M = 2$.

B. CALCULATIONS OF C_{42} for ASK, PSK, QAM

For ASK, PSK, and QAM, due to the constellations' symmetry and the baseband modulated signals' randomness, with different WFRFT order offset $\Delta\alpha$, the corresponding values of the 2th-order cumulants remain unchanged, while the ones of the 3th-order or other odd order cumulants exhibit instability. Therefore, to achieve a better tradeoff between the computations' complexity and recognition effectiveness, we decide to realize the modulation recognition for the WFRFT-based systems by employing 4th-order cumulants(C_{42}).

In a matter of clarity, when calculating only C_{42} for different baseband modulation signals, X_{ASK}, X_{PSK} and X_{QAM}, we will skip the subscripts ASK, PSK, and QAM in Eq.(6), (7) and (8) respectively. In the following deductions, the calculation of C_{42} will be conducted for different baseband modulations.

1) C_{42} FOR ASK

According to [33], let X be a random variable, whose available value comes from $\boldsymbol{s}$ in Fig. 1. the 4th-order Cumulants of X, C_{42} is expressed by

$$C_{42}(X) = E\left[(XX^*)^2\right] - \left|E(X^2)\right|^2 - 2\left[E(XX^*)\right]^2, \qquad (13)$$

where $E(\cdot)$, $|\cdot|$, $(\cdot)^*$, and $(\cdot)^2$ denote the expected value, the magnitude, the conjugate value, and square of the signal respectively.

According to the constellation distribution of Fig. 2(a), the constellation points are evenly distributed in the horizontal axis. For the sake of clarity, we only take the positive axis into consideration. Then C_{42} for ASK can be derived as follows

$$\begin{aligned} C_{42}(X) &= E\left[(XX^*)^2\right] - \left|E(X^2)\right|^2 - 2\left[E(XX^*)\right]^2 \\ &= \frac{2}{M}\sum\nolimits_{m=M/2}^{M-1}(2m+1-M)^4 \cdot d^4 \\ &\quad - \left(\frac{2}{M}\sum\nolimits_{m=M/2}^{M-1}(2m+1-M)^2\right)^2 \cdot d^4 - 2S^2. \end{aligned} \qquad (14)$$

According to the statistical theory, we can easily deduce that $E(XX^*)$ equals to the average power of $\boldsymbol{s}$. After substituting Eq.(10) into Eq.(14), we can get the following expression

$$C_{42}(X) = \left(\frac{3[3L^3+12L^2+8L-8]}{5(L+2)^2L} - 3\right)S^2, \qquad (15)$$

where $L = M-1$. More detailed deduction about Eq.(14) will be given in Appendix A. With $M = 4, 8, 16, \ldots$, in Eq.(15), $C_{42}(X)$ varies in the range $[-2, -1.2]S^2$. And when M gets larger, $C_{42}(X)$ gets closer to $-1.2S^2$.

2) C_{42} for PSK

As shown in Fig. 2(b), the constellation points of PSK are evenly distributed on the boundary line of a circle, then we only pay our attention to the first quadrant of Fig. 2(b). $E[(XX^*)^2]$ can be calculated as follows

$$E[(XX^*)^2] = \frac{4}{M}\sum\nolimits_{i=0}^{M/4-1}(x_i^2+y_i^2)^2. \qquad (16)$$

According to Eq.(11), $x_i^2 + y_i^2 = r^2$. After substituting Eq.(11) into Eq.(16), we can obtain the following expression

$$E[(XX^*)^2] = \frac{4}{M}\sum_{i=0}^{M/4-1}(r^2)^2 = r^4. \tag{17}$$

Considering that S is the average power of the baseband signal, we can deduce that $r^2 = S$. We can find that $\left|E(X^2)\right|^2 = 0$ due to the strict symmetry of the constellation in Fig. 2(b). $E[(XX^*)^2]$ is equal to the square of average power of $\boldsymbol{s}$, $E[(XX^*)^2] = S^2$. Then we can easily obtain C_{42} for PSK as follows

$$\begin{aligned} C_{42}(X) &= E\left[(XX^*)^2\right] - \left|E(X^2)\right|^2 - 2\left[E(XX^*)\right]^2 \\ &= (1-2)\cdot S^2 = -S^2. \end{aligned} \tag{18}$$

3) C_{42} for QAM

As for QAM, considering that QAM has a strict symmetric constellation, we only pay our attention to the first quadrant. Through baseband modulation, $\boldsymbol{c}$ is transformed into $\boldsymbol{s}$, according to Eq.(8), we can obtain the following expression

$$s_i = \sqrt{S}(x_i + jy_i),\ x_i, y_i \in (2m-1-\sqrt{M})d, \tag{19}$$

where, x_i and y_i are the real and imaginary part of the complex signal respectively.

According to Eq.(12), $d = \sqrt{3/(2(M-1))}$. In the first quadrant, there are $M/4$ constellation points. In the form of matrix, the magnitude square of each element in the constellation is expressed in (20), as shown at the bottom of this page. Then $E[(XX^*)^2]$ can be calculated by

$$E[(XX^*)^2] = \frac{4}{M}\cdot\sum_{i=\sqrt{M}/2+1}^{\sqrt{M}}\sum_{j=\sqrt{M}/2+1}^{\sqrt{M}}(x_i^2+x_j^2)^2 d^4. \tag{21}$$

After substituting Eq.(20) into Eq.(21), $E[(XX^*)^2]$ can be calculated through summation operations

$$E[(XX^*)^2] = \frac{7(H+1)^2-13}{5H(H+2)}S^2, \tag{22}$$

where $H = \sqrt{M} - 1$. More detailed deduction about Eq.(22) will be given in Appendix B.

We can also find that $\left|E(X^2)\right|^2 = 0$ due to the strict symmetry of the constellation in Fig. 2(c). Considering that $[E(XX^*)]^2 = S^2$, depending on Eq.(13), we can work out the value of C_{42} as follows

$$\begin{aligned} C_{42}(X) &= E\left[(XX^*)^2\right] - \left|E(X^2)\right|^2 - 2\left[E(XX^*)\right]^2 \\ &= (E[(XX^*)^2] - 2)\cdot S^2, \end{aligned} \tag{23}$$

where $E[(XX^*)^2]$ corresponds to Eq.(22). With $M = 4, 16, 64, \ldots,$ in Eq.(23), $C_{42}(X)$ varies in the range $[-1, -0.6]S^2$. And when M gets larger, $C_{42}(X)$ gets closer to $-0.6S^2$.

C. OPTIMISATION OF α_r BY MINIMISING C_{42}

As for WFRFT modulation, when N is larger enough, we can regard $\boldsymbol{X}_0, \boldsymbol{X}_1, \boldsymbol{X}_2$ and $\boldsymbol{X}_3$ as four unrelated random variables. As depicted in Fig. 1, let $\boldsymbol{X}_0 = \boldsymbol{s}$. According to Eq.(1), $C_{42}(\boldsymbol{W}^{\Delta\alpha}\boldsymbol{s})$ can be calculated by

$$\begin{aligned} C_{42}(\boldsymbol{W}^{\Delta\alpha}\boldsymbol{s}) = |\omega_0|^4 C_{42}(\boldsymbol{X}_0) + |\omega_1|^4 C_{42}(\boldsymbol{X}_1) \\ +|\omega_2|^4 C_{42}(\boldsymbol{X}_2) + |\omega_2|^4 C_{42}(\boldsymbol{X}_3). \end{aligned} \tag{24}$$

Considering $\boldsymbol{X}_0$ and $\boldsymbol{X}_2$ have the same statistical properties [34], besides, $\boldsymbol{X}_1$ and $\boldsymbol{X}_3$ are the normalized DFT of X_0 and X_2 respectively, Then $\boldsymbol{X}_1$ and $\boldsymbol{X}_3$ are asymptotically Gaussian when N is large enough [24]. $C_{42}(\boldsymbol{X}_1)$ and $C_{42}(\boldsymbol{X}_3)$ approach zero because the HOC of Gaussian signal is equal to zero. Then we mainly focus on the summation of $|\omega_0|^4 C_{42}(\boldsymbol{X}_0)$ and $|\omega_2|^4 C_{42}(\boldsymbol{X}_2)$. Because $\boldsymbol{X}_0$ and $\boldsymbol{X}_2$ have the same distribution properties, we can define $\mathbb{C}$ as the value $C_{42}(\boldsymbol{X}_0)$, then $C_{42}(\boldsymbol{X}_0) = C_{42}(\boldsymbol{X}_2) = \mathbb{C}$. When the WFRFT order $\Delta\alpha$ is set, we can rewrite $C_{42}(\boldsymbol{W}^{\Delta\alpha}\boldsymbol{s})$ as follows

$$C_{42}(\boldsymbol{W}^{\Delta\alpha}\boldsymbol{s}) = (|\omega_0|^4 + |\omega_2|^4)\mathbb{C}. \tag{25}$$

After substituting Eq.(2) into Eq.(25), we can get the following functions

$$\begin{aligned} &C_{42}(\boldsymbol{W}^{\Delta\alpha}\boldsymbol{s}) \\ &= (|\omega_0|^4 + |\omega_2|^4)\cdot\mathbb{C} \\ &= \left(\begin{aligned} &\left|\cos\left[\frac{(\Delta\alpha-0)\pi}{4}\right]\cos\left[\frac{2(\Delta\alpha-0)\pi}{4}\right]\right|^4 \\ &+\left|\cos\left[\frac{(\Delta\alpha-2)\pi}{4}\right]\cos\left[\frac{2(\Delta\alpha-2)\pi}{4}\right]\right|^4 \end{aligned}\right)\cdot\mathbb{C} \\ &= 0.5\left[(\cos(\pi\Delta\alpha/2\,))^4 + (\cos(\pi\Delta\alpha/2\,))^6\right]\cdot\mathbb{C}. \end{aligned} \tag{26}$$

Then the optimization of Eq.(26) is equal to the optimization of the following functions

$$f(u) = (\cos(u))^4 + (\cos(u))^6, \tag{27}$$

where $u = \pi\Delta\alpha/2$.

We can solve the optimization of Eq.(27) by taking derivatives, and the first and second derivative of $f(u)$ are given by

$$f'(u) = -\sin(u)\left[4(\cos(u))^3 + 6(\cos(u))^5\right], \tag{28}$$

$$Q_1 = \begin{pmatrix} 1^2+1^2 & 1^2+3^2 & \cdots & 1^2+(\sqrt{M}-1)^2 \\ 3^2+1^2 & 3^2+3^2 & \cdots & 3^2+(\sqrt{M}-1)^2 \\ \vdots & \vdots & \vdots & \vdots \\ (\sqrt{M}-1)^2+1^2 & (\sqrt{M}-1)^2+3^2 & \cdots & (\sqrt{M}-1)^2+(\sqrt{M}-1)^2 \end{pmatrix}. \tag{20}$$

$$f''(u) = 12(\cos(u))^2(-\sin(u))^2 - 4(\cos(u))^4 + 30(\cos(u))^4(-\sin(u))^2 - 6(\cos(u))^6. \quad (29)$$

Let $f'(u) = 0$, and $f''(u) < 0$, we can get the optimal solution is $u = \pi\Delta\alpha/2 \ = 0$, i.e. the optimal solution for Eq.(26) is $\Delta\alpha = 0$. In addition, according to the theoretical analyses in Eq.(15), (18), and (23), $\mathbb{C}$ is a negative number. Thus, through the optimization of Eq.(26), when $\mathbb{C} < 0$, $C_{42}(\boldsymbol{W}^{\Delta\alpha}\boldsymbol{s})$ can reach the minimum at $\Delta\alpha = 0$. That's the reason why we can get the optimal α_r by minimizing the 4th-order Cumulants of the receiving signal, C_{42}.

IV. NUMERICAL RESULTS

We simulate our WFRFT-based system in Fig. 1, with block length $N = 4096$. The WFRFT order $\Delta\alpha$ is in [0, 1], with the searching step 0.03. Without loss of generality, we make $S = 1$, and $-S^2$ can be omitted to simplify the descriptions of Eq.(15), (18) and (23). And we define $\tilde{C}_{42} = C_{42}/(-S^2)$.

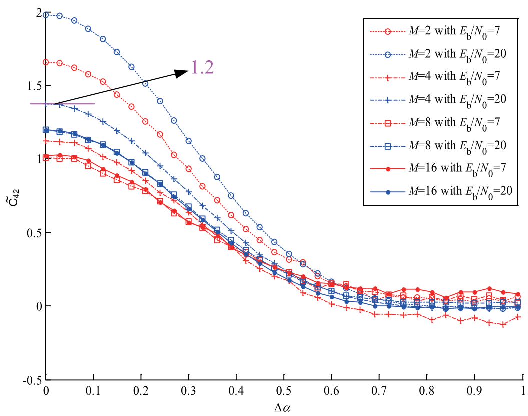

FIGURE 3. $\tilde{C}_{42}$ **of WFRFT-based systems for different parameters with ASK.**

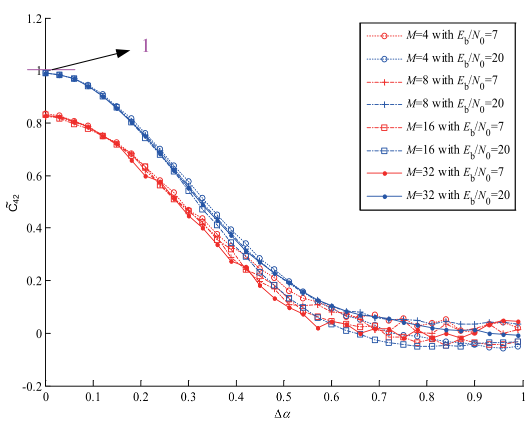

FIGURE 4. $\tilde{C}_{42}$ **of WFRFT-based systems for different parameters with PSK.**

As depicted in Fig. 3, we can observe that the system with a lager energy per bit-to-noise power spectrum density ratio (E_b/N_0) has a larger $\tilde{C}_{42}$ under the same baseband modulation order M. When E_b/N_0 is large enough ($E_b/N_0 > 20$), with the increase of M, $\tilde{C}_{42}$ in Fig. 3, Fig. 4

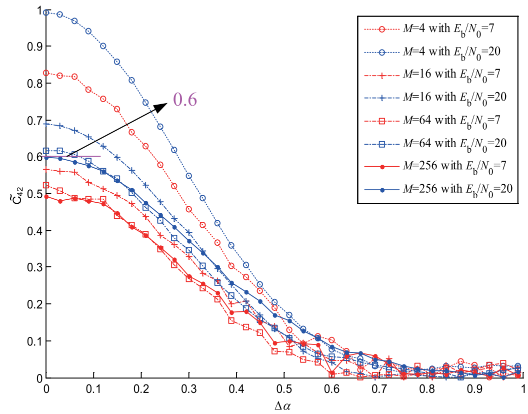

FIGURE 5. $\tilde{C}_{42}$ **of WFRFT-based systems for different parameters with QAM.**

and Fig. 5 approaches the theoretical boundaries 1, 1.2 and 0.6 respectively, which is consistent with Eq.(15), (18), and (23). We can find that when the WFRFT order $\Delta\alpha$ comes closer to 0, $\tilde{C}_{42}$ gets larger, which confirms that it's reasonable to get the optimal α_r by minimizing the 4th-order Cumulants of the receiving signal, C_{42} in Eq.(26). When $\Delta\alpha > 0.5$, $\tilde{C}_{42}$ gets smaller(approaching zero). That's because, in this situation($\Delta\alpha > 0.5$), the WFRFT-modulated signals exhibit strong Gaussian-like characteristics in Eq.(5). Besides, in view of the fact that the AWGN sequences have the pseudo-random characteristics and the OFDM signals have quasi-Gaussian distribution's characteristics, the values of $\tilde{C}_{42}$ will exhibit a slight fluctuation, to some extent, when the simulations are conducted under the situations with different noise's power σ^2 and DFT block length N. Thus, we can also find that there exists a slight fluctuation around zero when $\Delta\alpha$ is in [0.8, 1].

To explicitly exhibit how WFRFT order offset $\Delta\alpha$ can affect the received signals' characteristics, we also analyze the received signals' constellations with different $\Delta\alpha$ in the noiseless channel.

For the convenience of analyzing, we take 4QAM baseband modulation as an example to evaluate the related performances. Fig. 6(a),(b),(c) and (d) show the different constellations with $\Delta\alpha = 0$,0.3, 0.5, and 0.9 respectively. In Fig. 6, I and Q denote the Inphase and Quadrature parts of the constellation points. And the four different colored(red, blue, yellow, and green respectively) points denote the four different constellation sources originally generated from four quadrants in X-Y plane. As depicted in Fig. 6, with different $\Delta\alpha$, the constellations exhibit splitting and Gaussian-like characteristics. When $\Delta\alpha$ gets larger, the Gaussian-like characteristic gets stronger.

To further analyze the Gaussian-like characteristics for different $\Delta\alpha$, we evaluate the probability density function(PDF) of the received signals with different $\Delta\alpha$. According to the symmetric property of 4QAM and WFRFT, the real parts and imaginary parts of the WFRFT-modulated signal $W_k^{\Delta\alpha}s$ in Eq.(5) almost have the same statistical properties, so we only illustrate the PDFs for the real parts in Fig. 7. As shown

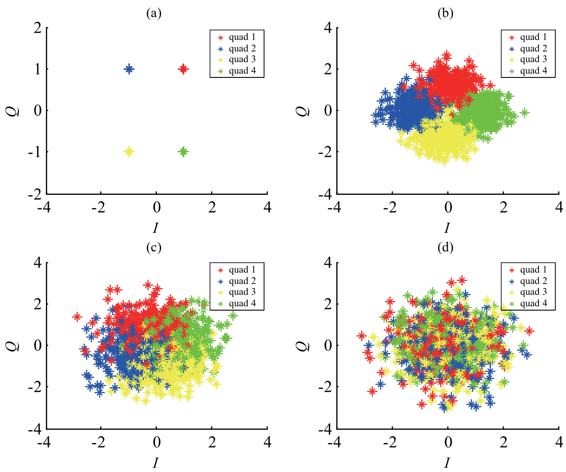

FIGURE 6. Diagram of the baseband modulation constellations for WFRFT signals with different $\Delta\alpha$.

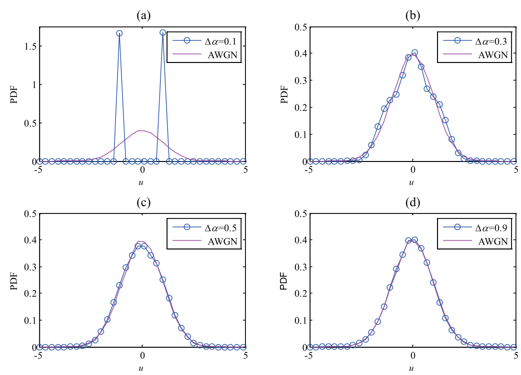

FIGURE 7. PDFs for the real parts of WFRFT signals with different $\Delta\alpha$.

in Fig. 7(a),(b),(c), and (d), when $\Delta\alpha$ gets larger, the contact ratio between the two PDF curves becomes higher in each subfigure. Especially, when $\Delta\alpha > 0.5$, the two PDF curves are almost the same, which demonstrates that the WFRFT signals can be almost regarded as Gaussian noise when $\Delta\alpha$ comes close to 1. And the law of the Gaussian-like characteristic along with $\Delta\alpha$ in Fig. 7 is consistent with the ones in Fig. 5 and Fig. 6.

In order to analyze the recognition performance of the designed systems, we also test the system's recognition rates with different baseband modulations. The adaptive thresholds are adopted to discriminate different modulation cardinalities. As shown in Fig.8, the system's recognition rates are larger than 90% at $E_b/N_0 > 6$. When E_b/N_0 is large enough ($E_b/N_0 > 11$), the values of C_{42} are easy to be discriminated(shown in Fig.3-5), and the recognition performances are almost the same(approaching 100%) for different modulation types and cardinalities. Considering the adaptive thresholds are selected depending on the actual relationship between the values of C_{42} and equivalent normalized AWGN signal's power, there doesn't exist a direct recognition performance comparison for different modulation types. Thus, for the same digital modulation types with different modulation cardinality M, when E_b/N_0 is small, for example, $E_b/N_0 < 5$,

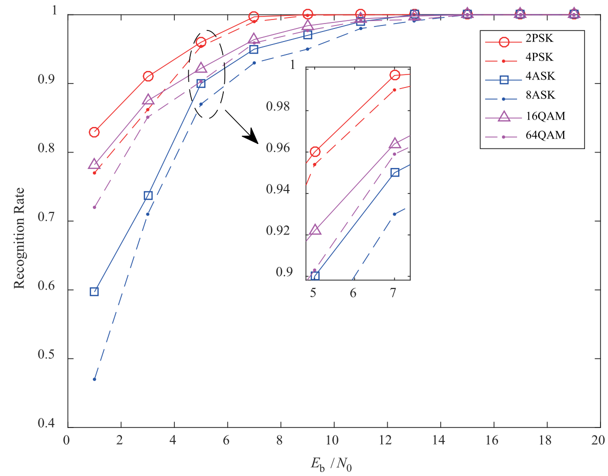

FIGURE 8. Recognition performances for WFRFT-based systems using C_{42}.

there exits an obvious recognition performance deterioration with the increase of M. And this mainly because the equivalent basis distance d(shown in Fig.2) will get smaller when the modulation cardinality M gets larger, which will finally lead to the degradation of the anti-AWGN capability based on the 4th-order cumulants(C_{42}).

V. CONCLUSION

In this paper, we conducted quantitative and qualitative analyses on the 4th-order Cumulants, C_{42} with ASK, PSK, and QAM for WFRFT-based systems. We put forward a novel modulation recognition and proved that the optimal α_r could be obtained by minimizing C_{42}, which could contribute to improving the system recognition performance. Future works will be done on the multiple parameters WFRFT-based system over other complex channels, such as multipath and double-selective channels.

APPENDIX A
DETAILED CALCULATION FOR EQ.(14)

Before deducing Eq.(14), we define the following summation formulas [35]

$$S_2(n) = \sum_{x=1}^{n} x^2 = \frac{n(n+1)(2n+1)}{6}, \tag{A.1}$$

$$S_4(n) = \sum_{x=1}^{n} x^4 = \frac{n(n+1)(2n+1)(3n^2+3n-1)}{30}, \tag{A.2}$$

where, we assume n is an odd number.

Then we can easily deduce the following formulas

$$S_{20}(n) = \sum_{x=1}^{(n-1)/2} (2x)^2 = \frac{n(n-1)(n+1)}{6}, \tag{A.3}$$

$$S_{40}(n) = \sum_{x=1}^{(n-1)/2} (2x)^4 = \frac{3n^5-10n^3+7n}{30}, \tag{A.4}$$

$$S_{21}(n) = S_2 - S_{20} = \frac{n(n+1)(n+2)}{6}, \tag{A.5}$$

$$S_{41}(n) = S_4 - S_{40} = \frac{3n^5 + 15n^4 + 20n^3 - 8n}{30}. \tag{A.6}$$

And let sum_1 denote the final value of the expression $E\left[(XX^*)^2\right] - \left|E(X^2)\right|^2$ in Eq.(14). Taking Eq.(A.5), (A.6) into consideration, we can rewrite sum_1 as

$$\begin{aligned} sum_1 &= \frac{2}{M}[1^4 + 3^4 + 5^4 + \cdots + (M-1)^4] \cdot d^4 \\ &\quad - \left(\frac{2}{M}[1^2 + 3^2 + 5^2 + \cdots + (M-1)^2]\right)^2 \cdot d^4 \\ &= \frac{2}{M} S_{41}(L) \cdot d^4 - \left(\frac{2}{M} S_{21}(L)\right)^2 \cdot d^4, \end{aligned} \tag{A.7}$$

where $L = M - 1$.

After substituting Eq.(10), (A.5) and (A.6) into Eq.(A.7), we can get the final expressions

$$\begin{aligned} sum_1 &= \frac{2}{M} \cdot \frac{L(L+1)(3L^3+12L^2+8L-8)}{30} \cdot \left(\frac{3}{M^2-1}\right)^2 \\ &\quad - \left(\frac{2}{M}\frac{L(L+1)(L+2)}{6}\right)^2 \cdot \left(\frac{3}{M^2-1}\right)^2 \\ &= \frac{3[3L^3 + 12L^2 + 8L - 8]}{5(L+2)^2 L} - 1. \end{aligned} \tag{A.8}$$

APPENDIX B
DETAILED CALCULATION FOR EQ.(22)

Let sum_2 denote the final value of the formula $(4/M) \cdot \sum_{i=\sqrt{M}/2+1}^{\sqrt{M}} \sum_{j=\sqrt{M}/2+1}^{\sqrt{M}} (x_i^2 + x_j^2)^2 \cdot d^4$. Then, we can rewrite sum_2 as follows

$$sum_2 = \frac{4}{M} \cdot d^4 \cdot \sum_{i=\sqrt{M}/2+1}^{\sqrt{M}} \sum_{j=\sqrt{M}/2+1}^{\sqrt{M}} (x_i^4 + x_j^4 + 2x_i^2 \cdot x_j^2). \tag{B.1}$$

After substituting Eq.(A.5), (A.6) into Eq.(B.1), we can deduce the following expression

$$\begin{aligned} sum_2 &= \frac{4}{M} \cdot d^4 \cdot \left\{ \begin{aligned} &2(\frac{\sqrt{M}}{2})[1^4 + 3^4 + \cdots + (\sqrt{M}-1)^4] \\ &+ 2([1^2 + 3^2 + \cdots + (\sqrt{M}-1)^2])^2 \end{aligned} \right\} \\ &= \frac{4}{M} \cdot d^4 \cdot \left\{ \begin{aligned} &2(\frac{\sqrt{M}}{2})\left[S_{41}(\sqrt{M}-1)\right] \\ &+ 2\left[S_{21}(\sqrt{M}-1)\right]^2 \end{aligned} \right\} \\ &= \frac{7(H+1)^2 - 13}{5H(H+2)}. \end{aligned} \tag{B.2}$$

where $H = \sqrt{M} - 1$.

ACKNOWLEDGMENT

The authors would like to thank the anonymous referees for their great constructive comments to improve our work.

REFERENCES

[1] C.-C. Shih, "Fractionalization of Fourier transform," *Opt. Commun.*, vol. 118, nos. 5–6, pp. 495–498, 1995.

[2] L. Mei, X.-J. Sha, and N.-T. Zhang, "The approach to carrier scheme convergence based on 4-weighted fractional Fourier transform," *IEEE Commun. Lett.*, vol. 14, no. 6, pp. 503–505, Jun. 2010.

[3] L. Mei, X. Sha, Q. Zhang, and N. Zhang, "The concepts of hybrid-carrier scheme communication system," in *Proc. Int. ICST Conf. Commun. Netw. China*, Aug. 2011, pp. 26–33.

[4] X. J. Sha, X. Qiu, and L. Mei, "Hybrid carrier CDMA communication system based on weighted-type fractional Fourier transform," *IEEE Communication Lett.*, vol. 16, no. 4, pp. 432–435, Apr. 2012.

[5] K. Wang, X. Sha, and L. Mei, "On interference suppression in doubly-dispersive channels with hybrid single-multi carrier modulation and an MMSE iterative equalizer," *IEEE Wireless Commun. Lett.*, vol. 1, no. 5, pp. 504–507, Oct. 2012.

[6] Y. Liang, X. Da, and S. Wang, "On narrowband interference suppression in OFDM-based systems with CDMA and weighted-type fractional Fourier transform domain preprocessing," *KSII Trans. Internet Inf. Syst.*, vol. 11, no. 11, pp. 5377–5391, Nov. 2017.

[7] Q. Wang, X. Feng, and Y. Liang, "On narrowband interference suppression in TDCS with WFRFT preprocessing," *Math. Problems Eng.*, vol. 2018, Aug. 2018, Art. no. 1231792.

[8] Y. Liang, X. Da, H. Hu, R. Xu, L. Ni, and D. Zhai, "Narrowband interference suppression in a spreading WFRFT system and optimal order selection," in *Proc. 10th Int. Conf. Commun. Softw. Netw.*, Jul. 2018, pp. 21–25.

[9] S. Yu, H. Dai, K. Wu, G. Zhou, X. Cheng, and C. Xu, "Performance analysis for WFRFT-OFDM systems to carrier frequency offset in doubly selective fading channels," in *Proc. 6th Int. Conf. Intell. Control Inf. Process.*, Nov. 2015, pp. 6–10.

[10] Y. Liang, X. Da, R. Xu, and L. Ni, "Design of constellation precoding in MP-WFRFT based system for covert communications," *J. Huazhong Univ. Sci. Technol. (Nature Sci. Ed.)*, vol. 42, no. 6, pp. 72–78, Feb. 2018.

[11] Y. Liang and X. Da, "Analysis and implementation of constellation precoding system based on multiple parameters weighted-type fractional Fourier transform," *J. Electron. Inf. Technol.*, vol. 40, no. 4, pp. 825–831, Jan. 2018.

[12] Y. Liang, X. Da, R. Xu, L. Ni, D. Zhai, and Y. Pan, "Secure communication using scramble phase assisting WFRFT," *IEICE Trans. Commun.*, vol. 102, no. 4, pp. 779–789, Apr. 2019.

[13] X. Da, Y. Liang, H. Hu, R. Xu, L. Ni, D. Zhai, and Y. Pan, "Embedding WFRFT signals into TDCS for secure communications," *IEEE Access*, vol. 6, pp. 54938–54951, 2018.

[14] K. Lau, M. Salibian-Barrera, and L. Lampe, "Modulation recognition in the 868 MHz band using classification trees and random forests," *AEU-Int. J. Electron. Commun.*, vol. 70, no. 9, pp. 1321–1328, Sep. 2016.

[15] P. S. Thakur, S. Madan, and M. Madan, "Trends in automatic modulation classification for advanced data communication networks," *Int. J. Adv. Res. Comput. Eng. Technol. (IJARCET)*, vol. 4, no. 2, pp. 496–507, Feb. 2015.

[16] O. A. Dobre, A. Abdi, Y. Bar-Ness, and W. Su, "Survey of automatic modulation classification techniques: Classical approaches and new trends," *IET Commun.*, vol. 1, no. 2, pp. 137–156, Apr. 2007.

[17] Z. Zhu and A. K. Nandi, "Blind digital modulation classification using minimum distance centroid estimator and non-parametric likelihood function," *IEEE Trans. Wireless Commun.*, vol. 13, no. 8, pp. 4483–4494, Aug. 2014.

[18] H. L. P. Kumar and L. Shrinivasan, *Automatic Digital Modulation Recognition System Using Feature Extraction*. Singapore: Springer, 2017.

[19] D. Zhang, W. Ding, B. Zhang, C. Xie, C. Liu, J. Han, and H. Li, *Heterogeneous Deep Model Fusion for Automatic Modulation Classification*. [Online]. Available: https://www.preprints.org/manuscript/201801.0097/v1

[20] X. Yan, G. Feng, H.-C. Wu, W. Xiang, and Q. Wang, "Innovative robust modulation classification using graph-based cyclic-spectrum analysis," *IEEE Commun. Lett.*, vol. 21, no. 1, pp. 16–19, Jan. 2017.

[21] A. Swami and B. M. Sadler, "Hierarchical digital modulation classification using cumulants," *IEEE Trans. Commun.*, vol. 48, no. 3, pp. 416–429, Mar. 2000.

[22] E. Moser, M. K. Moran, E. Hillen, D. Li, and Z. Wu, "Automatic modulation classification via instantaneous features," in *Proc. Nat. Aerosp. Electron. Conf.*, Jun. 2015, pp. 218–223.

[23] S. A. Ghauri, I. M. Qureshi, and A. N. Malik, "A novel approach for automatic modulation classification via hidden Markov models and Gabor features," *Wireless Pers. Commun.*, vol. 96, no. 3, pp. 4199–4216, Oct. 2017.
[24] W. Akmouche, "Detection of multicarrier modulations using 4th-order cumulants," in *Proc. IEEE Mil. Commun. Conf.*, Oct./Nov. 1999, pp. 432–436.
[25] Y. Nie, X. Shen, S. Huang, Y. Zhang, and Z. Feng, "Automatic modulation classification based multiple cumulants and quasi-Newton method for MIMO system," in *Proc. IEEE Wireless Commun. Netw. Conf.*, Mar. 2017, pp. 1–5.
[26] P. Liu and P.-L. Shui, "A new cumulant estimator in multipath fading channels for digital modulation classification," *IET Commun.*, vol. 8, no. 16, pp. 2814–2824, 2014.
[27] Z. Xu and T. Fujii, "A modulation classification method in cognitive radios system using stacked denoising sparse autoencoder," in *Proc. IEEE Radio Wireless Symp.*, Jan. 2017, pp. 218–220.
[28] A. Smith, M. Evans, and J. Downey, "Modulation classification of satellite communication signals using cumulants and neural networks," in *Proc. Cognit. Commun. Aerosp. Appl. Workshop*, Jun. 2017, pp. 1–8.
[29] H. Feng, L. Mei, S. Xuejun, and N. Zhang, "Modulation recognition for hybrid carrier scheme based on weighted-type fractional Fourier transform," in *Proc. Int. ICST Conf. Commun. Netw. China*, Aug. 2011, pp. 381–383.
[30] S. Xu, *Signal System*. Beijing, China: Tsinghua Univ. Press, 2016.
[31] L. Liu and J. Xu, "A novel modulation classification method based on high order cumulants," in *Proc. Int. Conf. Wireless Commun., Netw. Mobile Comput.*, Sep. 2006, pp. 1–5.
[32] C. Fan, *Communication Theory*, 6th ed. Beijing, China: House of Electronics Industry, 2015.
[33] C. L. Nikias and J. M. Mendel, "Signal processing with higher-order spectra," *IEEE Signal Process. Mag.*, vol. 10, no. 3, pp. 10–37, Jul. 1993.
[34] Y. Liang, X. Da, R. Xu, L. Ni, D. Zhai, and Y. Pan, "Research on constellation-splitting criterion in multiple parameters WFRFT modulations," *IEEE Access*, vol. 6, pp. 34354–34364, 2018.
[35] K. Macmillan and J. Sondow, "Proofs of power sum and binomial coefficient congruences via Pascal's identity," *Amer. Math. Monthly*, vol. 118, no. 6, pp. 549–551, Jun. 2011.

YUAN LIANG received the B.Sc., M.A.Sc., and Ph.D. degrees in information and communication engineering from Air Force Engineering University, Xi'an, China, in 2012, 2014, and 2018, respectively, where he is currently a Teaching Assistant with the Aeronautics Engineering College. His research interests include intelligent signal processing, wireless communications, secure communications, optimization, and intelligent algorithm.

XIN XIANG received the B.Sc. and M.A.Sc. degrees from the Aeronautics Engineering College, Air Force Engineering University, Xi'an, China, and the Ph.D. degree in signal and information processing from Xidian University, China, in 2009. He is currently a Professor with the Aeronautics Engineering College, Air Force Engineering University. His current research interests include radio communication software defined radio and navigation technology.

YE SUN received the M.A.Sc. degree in communication and information engineering from Air Force Engineering University, where he is currently a Lecturer. His current research interests include communication and navigation, and integrated avionics.

XINYU DA received the B.Sc. degree from Xidian University, in 1983, the M.A.Sc. degree in communication and electronic system from the Air and Missile Defense College, in 1988, and the Ph.D. degree from the School of Marine Science and Technology, NPU, in 2007. He is currently a Professor with Yango University. His research interests include satellite communications, communication theory, signal processing, transform domain communication systems, and cognitive radio.

CONG LI received the B.Sc. degree in measuring and control instrument from the China University of Petroleum, China, in 2016. He is currently pursuing the master's degree in information and communications engineering with the Air Force Engineering University. His research interests include military aviation communications and multi-antenna diversity receiving technology.

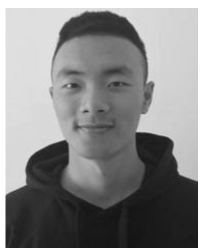

LIYAN YIN received the B.Sc. degree in information and communication engineering from Air Force Engineering University, Xi'an, China, in 2017, where he is currently a Graduate Student with the Aeronautics Engineering College. His research interests include software defined radio, communication signal processing, and system hardware design.